

RESEARCH

Open Access



Analysis of asymptomatic *Drosophila* models for ALS and SMA reveals convergent impact on functional protein complexes linked to neuro-muscular degeneration

Marina L. Garcia-Vaquero^{1,2}, Marjorie Heim³, Barbara Flix⁴, Marcelo Pereira¹, Lucile Palin³, Tânia M. Marques¹, Francisco R. Pinto¹, Javier de Las Rivas⁵, Aaron Voigt^{4,6}, Florence Besse³ and Margarida Gama-Carvalho^{1*}

Abstract

Background Spinal Muscular Atrophy (SMA) and Amyotrophic Lateral Sclerosis (ALS) share phenotypic and molecular commonalities, including the fact that they can be caused by mutations in ubiquitous proteins involved in RNA metabolism, namely SMN, TDP-43 and FUS. Although this suggests the existence of common disease mechanisms, there is currently no model to explain the resulting motor neuron dysfunction. In this work we generated a parallel set of *Drosophila* models for adult-onset RNAi and tagged neuronal expression of the fly orthologues of the three human proteins, named Smn, TBPH and Caz, respectively. We profiled nuclear and cytoplasmic bound mRNAs using a RIP-seq approach and characterized the transcriptome of the RNAi models by RNA-seq. To unravel the mechanisms underlying the common functional impact of these proteins on neuronal cells, we devised a computational approach based on the construction of a tissue-specific library of protein functional modules, selected by an overall impact score measuring the estimated extent of perturbation caused by each gene knockdown.

Results Transcriptome analysis revealed that the three proteins do not bind to the same RNA molecules and that only a limited set of functionally unrelated transcripts is commonly affected by their knock-down. However, through our integrative approach we were able to identify a concerted effect on protein functional modules, albeit acting through distinct targets. Most strikingly, functional annotation revealed that these modules are involved in critical cellular pathways for motor neurons, including neuromuscular junction function. Furthermore, selected modules were found to be significantly enriched in orthologues of human neuronal disease genes.

Conclusions The results presented here show that SMA and ALS disease-associated genes linked to RNA metabolism functionally converge on neuronal protein complexes, providing a new hypothesis to explain the common motor neuron phenotype. The functional modules identified represent promising biomarkers and therapeutic targets, namely given their alteration in asymptomatic settings.

Keywords ALS, SMA, Motor neuron, *Drosophila*, SMN, TDP-43, FUS, Transcriptomics, Network biology, Neurodegeneration

*Correspondence:

Margarida Gama-Carvalho
mhcarvalho@ciencias.ulisboa.pt

Full list of author information is available at the end of the article



© The Author(s) 2023. **Open Access** This article is licensed under a Creative Commons Attribution 4.0 International License, which permits use, sharing, adaptation, distribution and reproduction in any medium or format, as long as you give appropriate credit to the original author(s) and the source, provide a link to the Creative Commons licence, and indicate if changes were made. The images or other third party material in this article are included in the article's Creative Commons licence, unless indicated otherwise in a credit line to the material. If material is not included in the article's Creative Commons licence and your intended use is not permitted by statutory regulation or exceeds the permitted use, you will need to obtain permission directly from the copyright holder. To view a copy of this licence, visit <http://creativecommons.org/licenses/by/4.0/>. The Creative Commons Public Domain Dedication waiver (<http://creativecommons.org/publicdomain/zero/1.0/>) applies to the data made available in this article, unless otherwise stated in a credit line to the data.

Background

Motor neuron diseases (MNDs) are characterized by a progressive and selective degeneration and loss of motor neurons accompanied by an atrophy of innervated muscles. Although MNDs encompass heterogeneous groups of pathologies with different onset and genetic origins, a number of MND-causing mutations have been identified in RNA-associated proteins, leading to a model in which alteration of RNA metabolism may be a key, and potentially common, driver of MND pathogenesis [1–5]. This has become particularly clear in the context of two well-studied pathologies: Spinal Muscular Atrophy (SMA) and Amyotrophic Lateral Sclerosis (ALS), which have both been linked to mutations in conserved RNA binding proteins (RBPs). SMA, the most common early-onset degenerative neuromuscular disease, is caused in 95% of patients by a loss of the *SMN1* gene, which encodes a protein with chaperone functions essential for the assembly of both nuclear and cytoplasmic ribonucleoprotein (RNP) complexes [6, 7]. The best-characterized role of SMN is to promote the assembly of spliceosomal small nuclear ribonucleoprotein complexes (snRNPs) [8, 9], but it has also been involved in the assembly of other nuclear sRNPs required for 3'end processing [10], as well as cytoplasmic RNP complexes essential for long-distance mRNA transport [11, 12]. Consistent with these functions, and with additional reported roles in transcription regulation [13, 14], inactivation of SMN was shown to result in alternative splicing defects [15], transcriptional changes [16] and defective axonal RNA targeting [17, 18]. To date, how these changes in gene expression account for the full spectrum of symptoms observed in SMA patients and disease models remains unclear. ALS, on the other hand, is the most-common adult-onset MND and has mostly sporadic origins. Remarkably, however, disease-causing mutations in two genes encoding RNA binding proteins, FUS and TDP-43 (alias gene symbol of TARDBP), have been identified in both genetic and sporadic forms of the disease [4, 19]. Both proteins shuttle between the nucleus and the cytoplasm and regulate different aspects of RNA metabolism, ranging from transcription and pre-mRNA splicing to mRNA stability and axonal targeting [20–22]. ALS-causing mutations were described to have pleiotropic consequences, compromising both the nuclear and cytoplasmic functions of FUS and TDP-43, and resulting in their accumulation into non-functional cytoplasmic inclusions [2, 23]. Whether ALS pathogenesis primarily originates from a depletion of the nuclear pool of these RBPs, or rather from a toxic effect of cytoplasmic aggregates, has remained unclear [24, 25].

Thus, SMA and ALS are not only connected by pathogenic commonalities [26], but also appear to both

originate from alterations in RBP-mediated regulatory mechanisms. Further strengthening the possibility that these two MNDs may be molecularly connected, recent studies have suggested that SMN, FUS and TDP-43 belong to common molecular complexes and also exhibit functional interactions [27–33]. Together, these results have raised the hypothesis that SMN, FUS and TDP-43 may control common transcriptional and/or post-transcriptional regulatory steps. The alteration of these common processes in response to an impaired function of either protein would underlie MND progression [1]. Comparative transcriptomic studies performed so far, however, did not clearly identify classes of transcripts that may be co-regulated by the three MND RBPs [4, 34, 35]. This fact has left the question of the existence of common molecular regulatory mechanisms and targets in the diverse MNDs unanswered.

A major difficulty in comparing available transcriptomic studies is that the datasets were obtained from heterogeneous, and often late-stage or post-mortem samples. This prevents robust comparisons and the identification of direct vs. indirect targets. Another challenge associated with the identification of relevant regulated mRNAs is that SMN, FUS and TDP-43 are multifunctional and may exhibit distinct sets of target RNAs in the nucleus and the cytoplasm, raising the need for compartment-specific studies. To overcome previous limitations and unambiguously assess the existence of transcripts commonly regulated by SMN, FUS and TDP-43, we decided in this study to systematically identify the direct and indirect neuronal RNA targets of these proteins. For this purpose, we defined a strategy involving the establishment of parallel schemes for tagged-protein expression to perform RNP complex purification, alongside neuron specific, adult-onset gene silencing of the *Drosophila* orthologs of *SMN*, *FUS* and *TARDBP*, identified by the gene symbols *Smn*, *caz* and *TBPH*, respectively.

Highlighting the conservation of protein functions from fly to human, expression of human FUS and TDP-43 proteins was shown to rescue the lethality induced upon inactivation of the corresponding fly genes [36]. Furthermore, *Drosophila* models based on expression of mutant human or *Drosophila* proteins that recapitulate the hallmarks of SMA and ALS, in particular motor neuron disabilities and degeneration, have been previously established [37–41]. Several of these models have been successfully used for large-scale screening and discovery of genetic modifiers [41–43].

Our study was performed on asymptomatic flies starting from head samples. RNA immunoprecipitation sequencing (RIP-seq) experiments were performed to identify the cytoplasmic and nuclear transcripts bound by each protein. These assays were complemented with

neuron-specific, adult-onset down-regulation of *Smn*, *caz* or *TBPH* followed by RNA sequencing (RNA-seq) to identify transcripts with altered expression levels and/or splicing patterns. The RIP-seq analysis showed that the three proteins bind to largely distinct sets of RNA targets, in the nucleus and in the cytoplasm. Directly bound mRNAs were not particularly affected by the gene knockdowns, which collectively altered the expression and/or splicing profile of a limited, albeit significant set of common transcripts. These transcripts do not seem to be direct RNA-binding targets and do not present any consistent functional signatures. These observations suggested that the common physiological processes regulated by the three proteins may be altered at a higher order level. To unravel a possible functional relationship between transcripts regulated by *Smn*, *Caz* and *TBPH*, we designed a strategy to map them on neuronal protein complexes. Our results revealed a convergent effect of the three knockdowns on the regulation of common functional modules. Among these modules, we identified seven functional units directly implicated in neuro-muscular junction (NMJ) development. Noteworthy, although these modules were selected by suffering a common impact in all knockdowns, they were also found to be enriched in direct targets identified in RIP-seq experiments. Finally, selected functional modules were enriched in orthologues of human MND-associated genes. In summary, our work provides a new conceptual framework to explain how changes in three ubiquitous proteins involved in RNA metabolism converge into molecular functions critical for MN processes, thereby leading to overlapping disease phenotypes.

Methods

Fly lines

The fly stocks used were obtained from the Bloomington *Drosophila* Stock Center (BDSC) and the Vienna *Drosophila* Resource Center (VDRC), or were generated using the *Drosophila* Embryo Injection Service from BestGene (<http://www.thebestgene.com>). BDSC stocks #39,014 (expressing shRNA targeting *TBPH*), #55,158 (expressing shRNA targeting *Smn*) and #32,990 (expressing shRNA targeting *caz*) were used for the transcriptome profiling assays along with the VDRC strain #13,673 (expressing dsRNA targeting *always early*). Transgenic lines used for neuronal expression of GFP-tagged variants of *Smn* (CG16725, fly *SMN*), *TBPH* (CG10327, fly *TARDBP*), *caz* (CG3606, fly *FUS*) were generated by site directed integration into the same attP landing site (VK00013, BDSC#9732).

Smn, *caz* and *TBPH* coding sequences were PCR-amplified from ESTs LD23602, UAS-*caz* plasmid (gift from C. Thömmes) and EST GH09868, respectively.

Primers used for amplification are described in [Supplementary information](#). *Smn* and *caz* PCR products were subcloned into pENTR-D/TOPO vector (Life Technologies), fully sequenced, and recombined into a pUAS-EGFP-attB Gateway destination vector to express N-terminally-tagged proteins. The *TBPH* PCR product was double digested with NotI and XhoI and ligated into a NotI/XhoI digested pUAS-EGFP-attB plasmid (gift from S. Luschnig). Primer sequences are provided in [Supplementary information](#).

Fly crosses

shRNA expression was induced using the GeneSwitch system. Mifepristone was dissolved in 80% ethanol and pipetted on the surface of regular fly food (final concentration of 0,1 mg/cm²). Vehicle-only treated fly vials served as control. Vials were prepared 24 h prior to use to allow evaporation of ethanol. Crosses performed for 'knockdown' analyses were as follows: virgins carrying the ubiquitous daughterless GeneSwitch driver (*daGS*) were crossed with males carrying the UAS:shRNA constructs. In the progeny, male *daGS*/UAS:shRNA flies were collected one day post eclosion (1 dpe) and exposed to food containing mifepristone (replaced every 2nd day). After 10 days, flies were collected, snap frozen in liquid nitrogen and stored at -80 °C until further use. Knockdown efficiency of the target genes was assessed by RT-qPCR using *rp49* and *act5C* as normalizing genes using the primers listed in [Supplementary Information](#). The iScript[™] cDNA Synthesis Kit (BioRad) was used to transcribe 500 ng of total head RNA according to manufacturer's instructions. Real Time PCR was performed in a total reaction volume of 25 µL using the SYBR[™] Green PCR Master Mix (ThermoFisher).

For RIP-seq experiments, males carrying UAS-GFP-fusions (or sole EGFP) were crossed en masse with *elav-Gal4*; *tub-Gal80ts* virgins. *elav-Gal4/Y/+*; *tub-Gal80ts/UAS-GFP-Smn* (or *TBPH* or *caz*) flies were raised at 18 °C, switched to 29 °C upon eclosion and aged for 5 to 7 days before being collected in 50 mL Falcon tubes and snap frozen.

Immuno-histochemistry and western-blotting

For analysis of GFP-fusion distribution, brains were dissected in PBS and immuno-stained using anti-GFP antibodies (1:1,000; Molecular Probes, A-11122), as described previously [44]. Samples were imaged on an inverted Zeiss LSM710 confocal microscope. For analysis of GFP-fusion expression, heads were smashed into RIPA buffer (15 heads for 100 µL RIPA) and lysates directly supplemented with SDS loading buffer (without any centrifugation). Total protein extracts or RIP extracts were subjected to SDS Page electrophoresis, blotted to PVDF

membranes, and probed with the following primary antibodies: rabbit anti-GFP (1:2,500; #TP-401; Torey Pines); mouse anti-Tubulin (1:5,000; DM1A clone; Sigma); and mouse anti-Lamin (1:2,000; ADL 67.10 and ADL 84.12 clones; DHSB).

RNA Immunoprecipitation assays

Falcon tubes with frozen flies were chilled in liquid nitrogen and extensively vortexed to separate heads, legs and wings from the main body. Head fractions were collected at 4 °C, through sieving on 630 µm and 400 µm sieves stacked on top of each other. 1 mL of heads was used per condition, except for GFP-Smn, where 2 mL of heads were used. For the GFP control, 500 µL of heads were mixed with 500 µL of w¹¹¹⁸ heads to normalize the amount of GFP proteins present in the initial lysate.

Adult *Drosophila* heads were ground into powder with liquid nitrogen pre-chilled mortars and pestles. The powder was then transferred to a prechilled 15 mL glass Dounce Tissue Grinder and homogenized in 8.5 mL of Lysis buffer (20 mM Hepes pH 8, 125 mM KCl, 4 mM MgCl₂, 0.05% NP40, 1 mM dithiothreitol (DTT), 1:100 HaltTM Protease & Phosphatase Inhibitor Cocktail, Thermo Scientific, 1:200 RNasOUTTM, Invitrogen). Cuticle debris were eliminated by two consecutive centrifugations at 100 g for 5 min at 4 °C. Nuclear and cytoplasmic fractions were then separated by centrifugation at 900 g for 10 min at 4 °C. The supernatant (cytoplasmic fraction) was further cleared by two consecutive centrifugations at 16,000 g for 20 min. The pellet (nuclear fraction) was washed with 1 mL of Sucrose buffer (20 mM Tris pH 7.65, 60 mM NaCl, 15 mM KCl, 0.34 M Sucrose, 1 mM dithiothreitol (DTT), 1:100 HaltTM Protease & Phosphatase Inhibitor Cocktail, Thermo Scientific, 1:200 RNasOUTTM, Invitrogen), centrifuged at 900 g for 10 min at 4 °C and resuspended in 2 mL of Sucrose buffer. 800 µL of High salt buffer (20 mM Tris pH 7.65, 0.2 mM EDTA, 25% Glycerol, 900 mM NaCl, 1.5 mM MgCl₂, 1 mM dithiothreitol (DTT), 1:100 HaltTM Protease & Phosphatase Inhibitor Cocktail, Thermo Scientific, 1:200 RNasOUTTM, Invitrogen) were then added to reach a final concentration of 300 mM NaCl. After 30 min incubation on ice, the nuclear fraction was supplemented with 4.7 mL of Sucrose buffer to reach a concentration of 150 mM NaCl and with CaCl₂ to reach a 1 mM CaCl₂ concentration. RNase free DNase I (AmbionTM, Invitrogen) was added (0.1 mM final concentration) and the sample was incubated for 15 min at 37 °C with gentle agitation. EDTA was added to a 4 mM final concentration to stop the reaction, and the digested fraction was centrifuged at 16,000 g for 20 min (4 °C) to obtain soluble (supernatant; used for immuno-precipitation) and insoluble (pellet) fractions.

Cytoplasmic and nuclear fractions were incubated for 30 min at 4 °C under agitation with 120 µL of control agarose beads (ChromoTek, Germany). Pre-cleared lysates were collected by a centrifuging 2 min at 400 g (4 °C). Immuno-precipitations (IPs) were performed by addition of 120 µL of GFP-Trap[®]_A beads (ChromoTek, Germany) to each fraction and incubation on a rotator for 1.5 h at 4 °C. Tubes were then centrifuged for 2 min at 2,000 rpm (4 °C) and the unbound fractions (supernatants) collected. Beads were washed 5 times with Lysis buffer, resuspended in 100 µL of Lysis buffer supplemented with 30 µg of proteinase K (Ambion) and incubated at 55 °C for 30 min. Eluates (bound fractions) were then recovered and further processed. At least three independent IPs were performed for each condition.

RNA extraction, library preparation and RNA sequencing

RNA from IP eluates or frozen fly heads (50 flies approx/genotype) was extracted using Trizol according to the manufacturer's instructions. RIP-Seq libraries were prepared in parallel and sequenced at the EMBL Genomics core facility. Briefly, libraries were prepared using the non-strand-specific poly(A)+RNA Smart-Seq2 protocol (Nextera XT part). Following quality control, cDNA libraries were multiplexed and sequenced through single-end 50 bp sequencing (HiSeq 2000, Illumina).

For the RNA-preparation used in RNA-Seq experiments, 30–50 fly heads were homogenized in 0.5 ml Trizol (ThermoFischer) using a speed mill (Analytic Jena) and ceramic beads. Debris was removed by short centrifugation and supernatant was transferred to a fresh Eppendorf tube and incubated at 10 min on ice. 0.2 ml Chloroform were added and mixture was vortexed for 15 s and incubated on ice for 10 min followed by centrifugation for 15 minutes, 17,000 xg at 4 °C. Upper phase was removed and volume determined. RNA was precipitated by addition of 1× volume Isopropanol and incubated on ice for 1 h followed by a centrifugation for ten minutes with 17,000 xg at 4 °C. Supernatant was removed and pellet was washed twice with 1 ml ice cold 70% ethanol, air dried and resuspended in 25 µl RNase free water.

RNA-seq libraries for shRNA analysis were prepared and sequenced at the Genomics Facility, Interdisziplinäres Zentrum für Klinische Forschung (IZKF), RWTH Aachen, Germany. Libraries were generated using the Illumina TrueSeqHT library protocol and ran on a NextSeq machine with paired-end sequencing and a read length of 2×76nt. The 47 raw fastq files of the RNA-seq data generated for this study have been submitted to the European Nucleotide Archive under the umbrella project FlySMALS, with accession numbers PRJEB42797 and PRJEB42798.

RNA-seq data analysis

Following quality assessment using FastQC version 0.11.5 (<https://www.bioinformatics.babraham.ac.uk/projects/fastqc/>), all raw sequencing data was processed with in-house perl scripts to filter out reads with unknown nucleotides, homopolymers with length ≥ 50 nt or an average Phred score < 30 , and trim the first 10 nucleotides [45]. Remaining reads were aligned to the BDGP *D. melanogaster* Release 6 genome assembly build [46] using the STAR aligner version 2.5.0 [47] with the following options: `-outFilterType BySJout -alignSJoverhangMin 8 -alignSJDBoverhangMin 5 -alignIntronMax 100,000 -outSAMtype BAM SortedByCoordinate -twopassMode Basic -outFilterScoreMinOverLread 0 -outFilterMatchNminOverLread 0 -outFilterMatchNmin 0 -outFilterMultimapNmax 1 -limitBAMsortRAM 10000000000 -quantMode GeneCounts`. Gene counts were determined using the htseq-count function from HTseq (version 0.9.1) in union mode and discarding low quality score alignments (`-a 10`), using the Flybase R6.19 annotation of gene models for genome assembly BDGP6.

For RIP-seq data analysis, gene counts were normalized and tested for DE using the DESeq2 [48] package of the Bioconductor project [49], following removal of genes with less than 10 counts. mRNAs associated with each protein were identified by performing a differential expression analysis (DEA) for each condition vs the corresponding control pull-down. Transcripts with a positive log₂ FC and an adjusted *p* value for DEA lower than 0.05 were considered to be bound by the target protein.

DEA for RNA-Seq gene counts was performed with the limma Bioconductor package [50] using the voom method [51] to convert the read-counts to log₂-cpm, with associated weights, for linear modelling. The design formula (`~ hormone + Cond`, where `hormone = treated` or `non-treated` and `Cond = Caz, Smn` or `TBPH RNAi`) was used to consider hormone treatment as a batch effect. Differential gene expression analysis was performed by comparing RNAi samples for each target protein to control (always early RNAi) samples. Genes showing up or down-regulation with an adjusted *p* value < 0.05 were considered to be differentially expressed.

Altered splicing analysis (ASA) was performed on the RNA-seq aligned data using rMATS version 4.0.2 [52] with flags `-t paired -nthread 10 -readLength 66 -libType fr-firststrand`. For the purpose of the downstream analysis, the union of all genes showing any kind of altered splicing using the junction count and exon count (JCEC) analysis with a FDR < 0.05 in the comparison between each target gene RNAi versus control RNAi was compiled as a single dataset.

Normalized RNA-Seq data of adult fly brain tissue was retrieved from FlyAtlas2 database in November 2020

(www.flyatlas2.org; [53]). Neuronal transcripts were filtered applying an expression threshold of > 1 FPKM (Fragments Per Kilobase per Million). This gene set was then used to filter the final gene lists from RIP-seq, DEA and ASA. The full universe of 8,921 neuronal genes is annotated in Supplementary Data 5.

Clustering analysis was performed using the heatmap function from ggplot2 R package (default parameters) [54] and correlation plots were generated using lattice R package. Intersection analyses of RNA-Seq and RIP-seq datasets were performed using UpSetR and SuperExact-Test R packages [55].

Network analysis and generation of the library of functional modules

Drosophila physical Protein–Protein Interaction (PPI) data was retrieved from APID repository (<http://apid.dep.usal.es>; [56, 57] in December 2019. The original unspecific network was filtered to include only interactions between proteins expressed in adult fly brain tissue as described in previous section. The neuronal network was then simplified to remove self-loops and isolated proteins using the igraph R package [58]. Bioconductor GOfuncR R package [59] was used to evaluate the functional enrichment of brain network as compared to the unspecific network—Gene Ontology Biological Process, hyper-geometric test, FDR = 0.1 on 1000 randomizations. Finally, the functional modules were defined by selecting groups of physically interacting proteins annotated under the same enriched term. It should be noted that not all the proteins collaborating in the same process must physically interact (*e.g.*, as in the case of cell signaling, the membrane receptor does not bind to its downstream transcription factor). Based on this, we enabled modules to be formed by non-connected subnetworks. The isolated clusters were discarded only when the largest subnetwork represented more than 90% of the total module. The same protein might be annotated with several terms and therefore might be involved in several modules simultaneously. Conversely, we are aware that the use of GO data may return functionally redundant modules. Prior any further analysis, module redundancy was evaluated to check that modules do not exceedingly overlap nor represent redundant biological processes. Based on this analysis, a module size from 10 up to 100 proteins was defined as optimal to minimize redundancy.

Statistical analysis

In addition to the statistical methods described in the sections “RNA-seq data analysis” and “Network analysis and generation of the library of functional modules”, median values of two independent samples were compared with the Wilcoxon-Mann-Whitney test (using the

wilcox.test R function), while the Chi-square test (chisq.test R function) was used to compare two independent proportions. *P*-values lower than 0.05 were considered statistically significant.

Results

Caz, Smn and TBPH proteins do not share common mRNA targets

We hypothesized that the existence of shared RNA targets for Caz, Smn and TBPH might underlie the observed phenotypic commonalities between SMA and ALS. To test this hypothesis, we performed RIP-seq to identify neuronal mRNAs present in the RNP complexes formed by each of these proteins in adult *Drosophila* neurons. To facilitate cross-comparisons and ensure reproducible and cell-type specific purification, we generated three independent transgenic lines with GFP-tagged constructs expressed under the control of UAS sequences inserted into the same chromosomal position. To specifically characterize the neuronal RNA interactome, GFP-fusion proteins were expressed in adult neuronal cells using the pan-neuronal *elav*-GAL4 driver. The ectopic expression of Caz, Smn and TBPH has been reported to induce toxicity [60–62]. For this reason, we used the TARGET method [63] to express GFP-fusion proteins specifically in adult neurons within a limited time window (5–7 days post-eclosion). The TARGET system relies on the temperature-sensitive GAL80 protein, which inhibits GAL4 at low temperature, enabling temporal regulation of UAS constructs. When expressed in neuronal cells, GFP-Caz and GFP-TBPH robustly accumulated in the soma, showing a predominant, although not exclusive nuclear accumulation (Supplementary Fig. S1A and C). As expected, GFP-Smn was found mainly in the cytoplasm, sometimes accumulating in U bodies [64, 65] (Supplementary Fig. S1B). Despite the same insertion site and promotor

sequence, GFP-Smn protein was consistently expressed at lower levels (Supplementary Fig. S1D).

Since Caz, Smn and TBPH are multifunctional proteins involved in both nuclear and cytoplasmic regulatory functions, we separately characterized their RNA interactome in each cellular compartment. For this purpose, cellular fractionations were performed prior to independent anti-GFP immunoprecipitations, thus generating paired nuclear and cytoplasmic samples (Fig. 1A). As shown in Fig. 1B, relatively pure nuclear and cytoplasmic fractions were obtained from head lysates and GFP-tagged proteins could be efficiently immuno-precipitated from each fraction.

For each paired nuclear and cytoplasmic pull-down, co-precipitated RNAs were extracted and used to prepare mRNA-seq libraries. Pull-downs from flies expressing GFP were used as control. Three independent replicate datasets were generated for each protein, except for GFP-Caz, for which one nuclear pull-down sample did not pass quality control for library generation. The raw sequencing dataset, composed of 23 libraries containing between 17.7 and 64.6 million total reads (Supplementary Data 1), was submitted to the European Nucleotide Archive (ENA) with the study accession code PRJEB42798.

RIP-seq datasets were analyzed to identify mRNA molecules enriched in GFP-fusion versus GFP control pull-downs with an average of 13,500 genes detected across all samples, ranging (Supplementary Data 1). Sequencing datasets clustered primarily depending on the nuclear *versus* cytoplasmic natures of the extract, and secondly depending on the protein used for pull-down (Supplementary Fig. S2A). Differential expression analysis (DEA) was performed between each of the six pull-down conditions and the corresponding GFP control, with transcripts displaying positive enrichment (adjusted *p* value < 0.05) considered as associating with the target protein (Supplementary Data 2).

(See figure on next page.)

Fig. 1 RIP-Seq identification of mRNAs bound by Caz, Smn or TBPH in adult *Drosophila* neurons. **A** Schematic representation of the RIP-Seq procedure. GFP-fusion proteins were conditionally expressed in the nervous system of adult flies via the Gal4/Gal80 ~ UAS system. Head lysates were prepared and fractionated into cytoplasmic and nuclear fractions (see Methods). Nuclear proteins were further solubilized with high salt buffer and recovered in the soluble fraction. The cytoplasmic and nuclear soluble fractions were used for immuno-precipitation with GFP-trap beads. Co-immunoprecipitated mRNAs were extracted and sequenced. **B** Western blot analysis of the different fractions obtained in the RIP procedure. Lamin and Tubulin were used as markers of the nuclear and cytoplasmic fractions, respectively. Depletion of Tubulin from the nuclear fraction and of Laminin from the cytoplasmic fraction demonstrates the quality of the fractionation procedure. Also note the differential distribution of GFP-Caz, Smn and TBPH in the different fractions. As expected, Smn was predominantly localized in the cytoplasmic fraction, and Caz in the nuclear. In contrast, TBPH was abundant in both fractions. **C** Bar graph showing the number of neuronal mRNAs co-immunoprecipitated with Caz, Smn or TBPH from cytoplasmic (blue) or nuclear (yellow) lysates. Transcripts found in both compartments are shown in green. **D** Venn diagrams illustrate the overlap between the total (top panel), cytoplasmic (middle panel) or nuclear (lower panel) mRNA interactomes of Caz, Smn and TBPH. The total mRNA interactomes (“All”) correspond to the union of interactions detected in the cytoplasm and in the nucleus. The seven transcripts found in the overlap of the top diagram (“All”) are not detected in the overlap of cytoplasmic and nuclear interactomes because they correspond to mRNA molecules present in distinct compartments

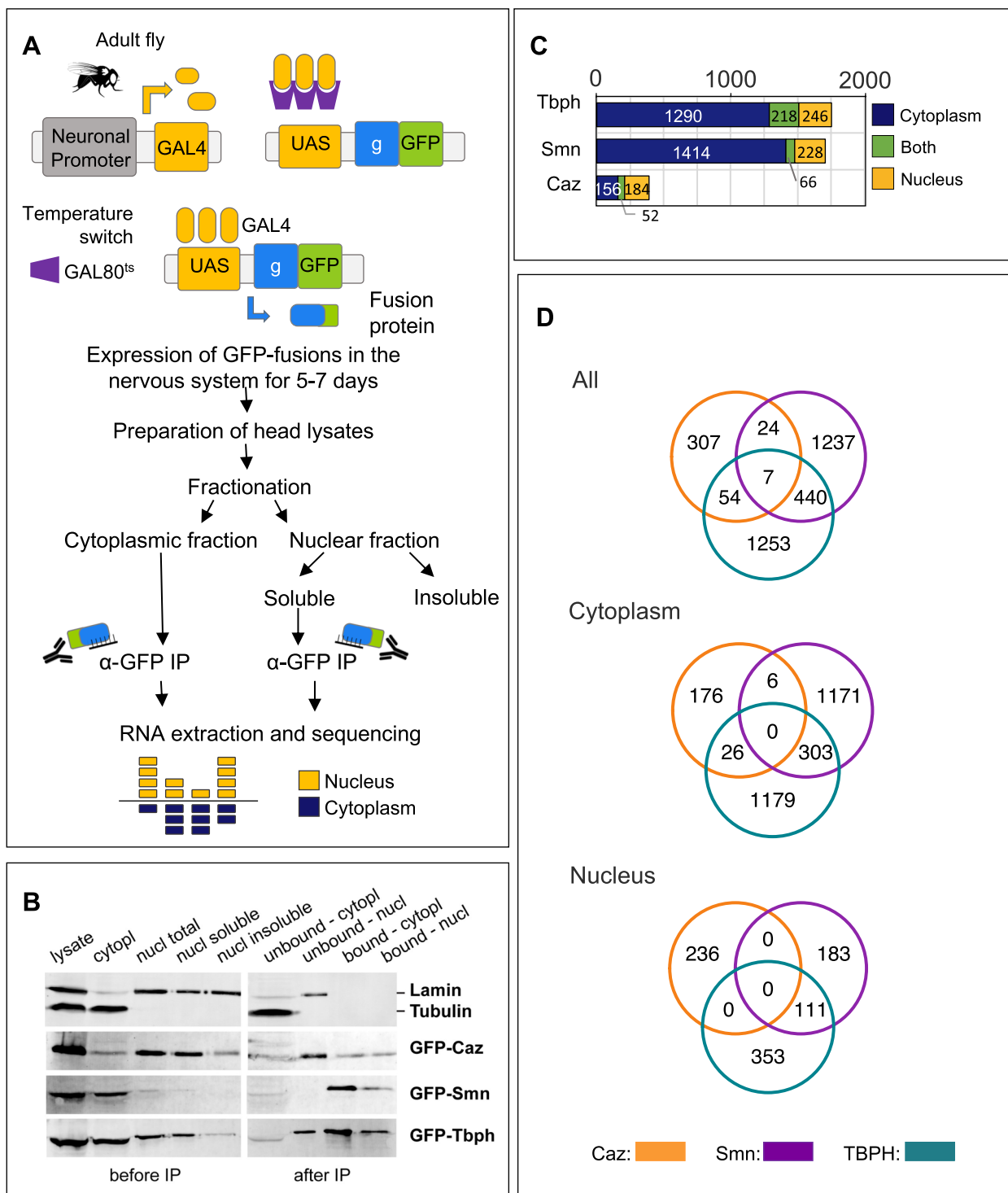


Fig. 1 (See legend on previous page.)

Although Caz, Smn and TBPH fusion proteins were expressed specifically in neurons via the *elav* promoter, a certain degree of RNP complex re-association may occur in head lysates during the different experimental steps, as previously described [66]. To discard any non-neuronal

transcripts that may have co-precipitated with target proteins, the dataset resulting from the DEA was filtered to include only genes with reported expression in the adult fly brain (see Methods), corresponding on average to 70% of the enriched transcripts (see Supplementary Fig. S3).

These analyses revealed that Smn and TBPH associate with a large fraction of the neuronal transcriptome (1,708 and 1,754 mRNAs in total, respectively), and that most of their identified mRNA targets associate in the cytoplasm rather than in the nucleus (Fig. 1C). A much smaller number (208) of mRNAs were found to associate with Caz in the cytoplasm, with 236 mRNAs detected as enriched in the pull-downs from nuclear fractions. Although this may partly reflect the higher heterogeneity of the Caz pull-down samples (Supplementary Fig. S2A), it is in good agreement with the low abundance of GFP-Caz protein found in the cytoplasm compared to GFP-Smn and GFP-TBPH (Fig. 1B). Of note, the percentage of transcripts simultaneously bound by the same protein on both compartments averaged only 22%, with TBPH displaying a much larger overlap than Smn for a similarly sized set of target mRNAs (Fig. 1C). This observation is in agreement with the current model of mRNP complex remodeling between the nucleus and the cytoplasm, with the compartment-specific set of mRNA bound proteins being influenced both by their relative affinities and abundance [66].

We next addressed the existence of common RNA targets, which could provide insights regarding a potential common MN degenerative mechanism associated with the altered expression of the human orthologue proteins in a disease context. Overlap analysis of the mRNA interactomes of Caz, Smn, and TBPH revealed a striking absence of transcripts bound by all three RBPs in the cytoplasmic or nuclear fractions (Fig. 1D). This finding might not exclusively result from the small number of RNAs bound by Caz, as a poor overlap was also observed between the large sets of cytoplasmic mRNAs bound by TBPH and Smn. Considering that the universe of protein-associated transcripts was defined exclusively based on the adjusted p value, without imposing a minimal enrichment threshold, this observation is particularly surprising. Together, our RIP-seq experiments thus uncovered that Caz, Smn and TBPH do not share common RNA targets.

Gene expression changes in response to reduced levels of Caz, Smn and TBPH have significant commonalities but lack a clear functional signature

In addition to regulatory roles associated with mRNA binding activity, Caz, Smn, and TBPH have been shown to have both direct and indirect roles as transcriptional, translational, and splicing regulators (reviewed in [4]). It is thus possible that, despite associating to non-overlapping sets of mRNAs, these proteins may coordinate common gene expression programs through other molecular mechanisms. To address this hypothesis, we used shRNA-expressing fly lines to knock-down the expression of *caz*, *Smn*, and *TBPH* in adult flies by RNA interference (RNAi) and characterized the resulting changes in neuronal gene expression using RNA-seq (Fig. 2A). After identification of fly lines displaying a robust silencing of each target gene, we used the GeneSwitch (GS) system to induce ubiquitous, adult-onset RNAi [67]. This system relies on the feeding of flies with the hormone mifepristone (RU486), which activates GAL4-progesterone-receptor fusions, thus driving expression of the shRNA transgenes (Fig. 2A). Given that the system has been reported to display some leakage in the absence of the hormone [68], a fly line expressing shRNA against the non-related embryonic transcript *always early* (*ae*) was used as control. Three to five days post-eclosion, resulting male progeny was transferred to food with or without the shRNA-inducing hormone for ten days and knock-down efficiency of target genes was evaluated by qRT-PCR (Supplementary Fig. S1E). Of note, despite an effective knock-down of the target gene levels of ~50%, these flies did not exhibit any motor phenotype or increased mortality. Therefore, our model represents an asymptomatic disruption of the molecular pathways regulated by the *caz*, *Smn* and *TBPH* genes. Total RNA extracted from fly heads from three independent experimental assays was used for library preparation and paired-end Illumina mRNA sequencing (RNA-seq). The raw sequencing dataset, composed of 24 libraries with an average number of

(See figure on next page.)

Fig. 2 Identification of differentially expressed neuronal transcripts in response to RNAi-mediated silencing of Caz, Smn or TBPH in adult flies.

A Schematic representation of the experimental set-up for RNA-seq analysis. Hormone-dependent, adult-onset expression of short hairpin (sh) RNA was used to induce RNAi-mediated gene silencing of *caz*, *Smn* or *TBPH*. RNA was prepared from fly heads five to seven days post induction of shRNA expression, quality checked and subjected to mRNA-seq. Fly lines with shRNA against the *always early* (*ae*) embryonic gene served as control. **B** Bar graph showing the RNA-seq log₂ fold change of the siRNA target genes plus the *Gapdh* housekeeping gene in each RNAi fly line. Statistically significant differences to the *ae* siRNA fly line are indicated as ** (adjusted p value < 0.05) and * (adjusted p value = 0.06 and p value < 0.02). **C** Bar graph showing the number of upregulated (red), downregulated (green) and differentially spliced mRNAs (yellow) in each RNA-seq dataset. Note that the kind of splicing change was not considered for this analysis. **D** Venn diagrams and corresponding bar graphs showing the overlap in upregulated (top), downregulated (middle) or differentially spliced (bottom) mRNAs in flies with RNAi-mediated silencing of *caz*, *Smn* or *TBPH*. The bar color compares the expected (black) and observed (red) overlap given the total transcripts altered in response to the silencing of *caz*, *Smn* or *TBPH*, respectively. The size of randomly expected overlaps and the statistical tests comparing observed with expected overlaps were calculated using the *SuperExactTest* R package. All shown overlaps are significantly larger than expected by chance (observed and expected overlap sizes and respective p-values are presented in Supplementary data file 5

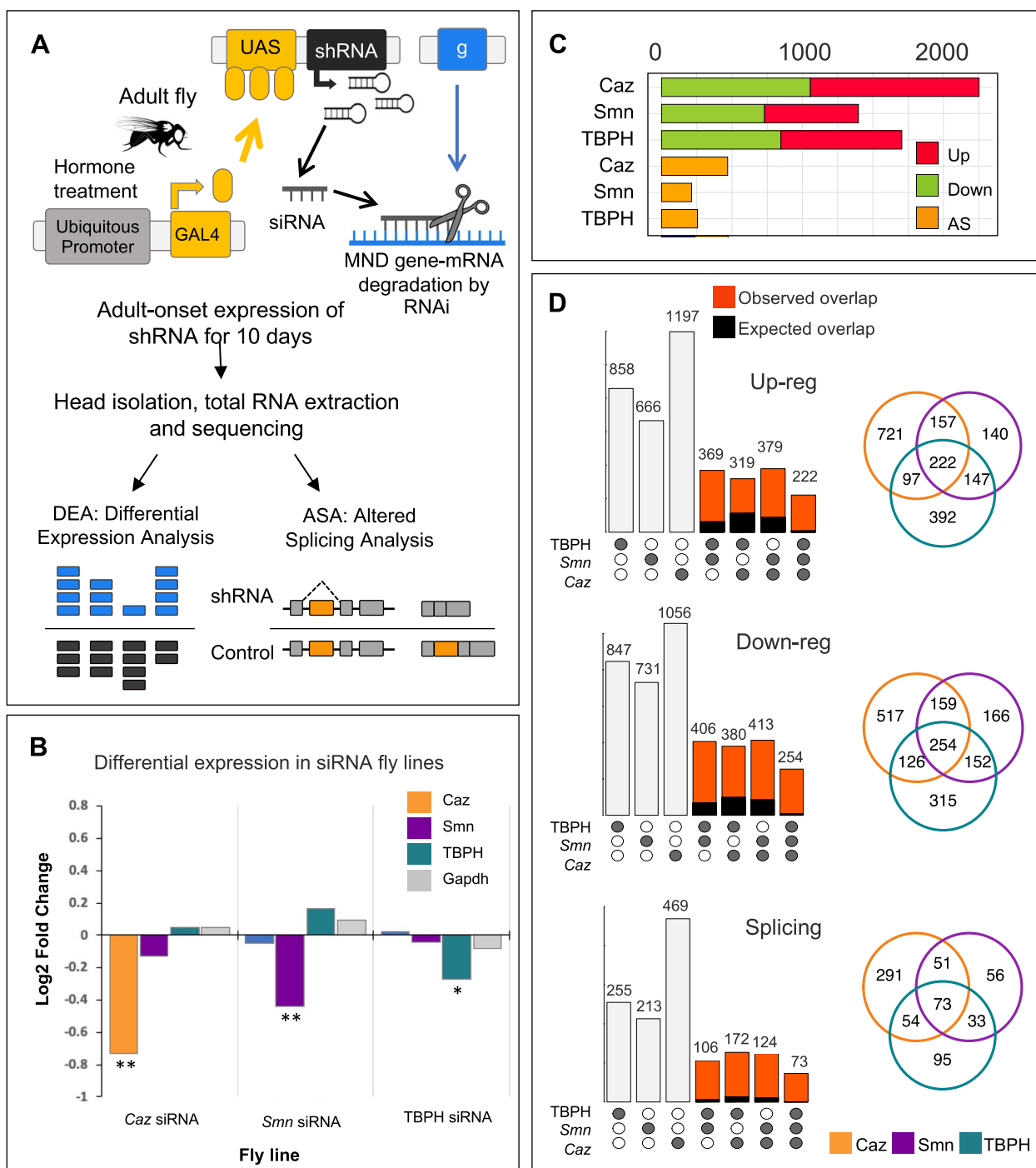


Fig. 2 (See legend on previous page.)

50 million reads (Supplementary Data 1), was submitted to ENA with the study accession code PRJEB42797.

Following quality control and filtering, reads were aligned to the *Drosophila* reference genome, mapping to ~13,600 expressed genes. The RNA-seq dataset was analyzed to determine the overall changes in

transcript abundance and splicing patterns induced by the knock-down of each protein. Exploratory analysis of the normalized RNA-seq dataset revealed that the samples clustered primarily according to genotype, followed by treatment (Supplementary Fig. S2B), an observation consistent with the expected leakage from

the siRNA locus. However, hormone-treated samples exhibited a better separation between genotypes than the corresponding untreated controls, as expected from shRNA-expressing samples (Supplementary Fig. S2C). As hormone treatment induced a significant number of common changes across all sample types, explaining up to 7% of the variance in the dataset (Supplementary Fig. S2C), differential gene expression (DE) analysis was performed between hormone treated *Caz*, *Smn* and *TBPH* shRNA-expressing target and control fly lines (see Supplementary Data 3). Confirming the robustness of our dataset and DE analysis, the specific shRNA target genes were found to be significantly down-regulated exclusively in the corresponding fly line (Fig. 2B). Given that our three target proteins are known to regulate mRNA processing, we also analyzed the data to identify alternative splicing (AS) changes that occurred as a consequence of the gene knockdowns (Supplementary Data 4). Although the analysis we performed distinguishes between five distinct types of AS, for the aim of the present study all AS changes identified in each siRNA line were combined and transcripts defined as either alternatively spliced, or not affected. Taking into consideration that RNA-seq was performed using samples isolated from fly heads, the list of transcripts showing significant DE or AS changes in response to *caz*, *Smn* or *TBPH* knock-down was filtered as previously described to exclude non-neuronal genes (Supplementary Fig. S3). Supplementary Data 5 provides the final annotated list of all neuronal genes detected in the different fly models and experiments.

Figure 2C summarizes the overall results of the RNA-seq analysis. Although the proportion of up- and down-regulated genes within the DE gene set (~50%) was similar in all conditions, there were considerable differences in the number of DE or AS transcripts identified in response to each knockdown (Fig. 2C). Given the correlation between these numbers and the observed knockdown efficiency and sample heterogeneity (Fig. 2B and Supplementary Fig. S2B), we believe these differences more likely reflect our experimental set-up than a specific characteristic of the gene expression programs regulated by each target protein. Importantly, only a relatively small fraction of the DE transcripts was identified as a direct protein target in the RIP-seq assays (Supplementary Data 5). *Caz*-regulated transcripts showed minimal direct association with *Caz* protein (4.6%), whereas ~22% of the genes showing altered expression in response to *Smn* or *TBPH* RNAi were found to be enriched in the corresponding RIP-seq assays. Interestingly, this fraction goes up to ~40% when considering only the transcripts displaying AS changes in response to *Smn* or *TBPH* knock-down, suggesting the splicing of

these transcripts may be directly regulated by each protein (Supplementary Data 5).

We next looked for the commonalities between the sets of transcripts with altered expression induced by the knockdown of each target protein. A summary of the number of genes displaying common changes in expression as a consequence of the shRNA knockdowns is depicted in Fig. 2D. The overlap analysis of these gene sets revealed that approximately 500 genes exhibit similar gene expression changes in response to all knockdowns (Fig. 2D). This is well above the overlap expected by random chance, with an estimated p value < 1e-16. Performing the overlap analysis for common DE genes without requiring that the type of change is identical in the three fly lines only retrieved an additional 20 genes, underscoring the significance of the common changes that were detected. Thus, despite the total lack of common RIP-seq targets, the downregulation of *Caz*, *Smn* and *TBPH* protein expression seems to elicit a coherent transcriptome response.

In an attempt to understand the functional consequences of this common transcriptome signature, we performed a functional enrichment analysis to identify altered biological processes. Surprisingly, almost no Gene Ontology (GO) terms were enriched in the subset of ~500 common genes (Supplementary Data 6). This result is in stark contrast with the strong functional signature that was observed for GO enrichment analysis of the subsets of mRNAs captured in the RIP-Seq assays. Furthermore, the identification of functional signatures was not improved by imposing more stringent fold change cut-offs on the DE gene sets. Indeed, the majority of DE genes showing common changes across all knockdowns presents very small variations in expression (Supplementary Fig. S2D). The use of more stringent fold change cut-offs on our dataset leads to a big reduction in the size of the gene sets (Supplementary Fig. S2E), with an even larger impact on the number of common DE genes that are retained (Supplementary Fig. S2F). These observations support our choice to consider all genes showing statistically significant changes in expression in our analysis, independently of their fold change level. However, we were unable to link this group of genes to a coherent set of molecular processes that are directly influenced by the three proteins, which might provide novel insights into the human disease context. Nevertheless, given the clear presence of a shared transcriptome signature, we hypothesized that putative underlying functional connections might be obscured by independent, albeit converging phenomena, taking place at the protein network level. To obtain insights into these potential connections, we proceeded to a more in-depth network-based analysis of our datasets.

Network-based approaches identify commonly affected neuronal functional modules

Biological processes are dynamic and complex phenomena that emerge from the interaction of numerous proteins collaborating to carry out specialized tasks. Thus, a biological process can be similarly impacted by changes in distinct proteins that contribute to the same regulatory function.

To understand whether the phenotypic commonalities observed in ALS and SMA might result from the deregulation of distinct, but functionally connected target proteins, we used a computational network-based approach. First, following our recently published approach [69], we generated a library of tissue-specific "functional modules" comprised of physically interacting and functionally collaborating neuronal proteins (Fig. 3A). To do so, we began by reconstructing the entire *Drosophila* neuronal interaction network using protein–protein interaction (PPI) and adult fly brain RNA-seq datasets available in the APID and FlyAtlas2 repositories, respectively [53, 56]. Notably, 45.5% of the 5 353 proteins found in this neuronal network are encoded by transcripts whose levels and/or splicing were altered in response to *caz*, *Smn* and/or *TBPH* knockdowns. Next, we defined functional modules in the neuronal network by selecting groups of physically interacting proteins annotated under the same enriched functional term. Of the 232 modules with associated GO terms, we focused on the subset of 122 modules composed of 10 to 100 proteins (Supplementary Data 7). These modules retained 1541 proteins in total, maintaining the high percentage of *Caz*, *Smn* and/or *TBPH*-dependent genes found in the original network (43.7%).

To evaluate the impact of each of the three proteins on individual functional modules, we calculated the percentage of nodes belonging to the DE or AS categories. To focus on modules simultaneously affected by the down-regulation of *caz*, *Smn* and *TBPH*, we assigned to each module an "overall impact" score, defined as the percentage of transcripts showing altered expression in the knockdown with the lowest impact (Fig. 3A). In this way, a functional module with an overall impact of X% has at least that percentage of nodes affected by any of the three knockdowns. 52 modules with an overall impact score of $\geq 20\%$ were identified. These modules were selected for further analysis, as they seem to be under the common control of all three proteins, although not necessarily through regulation of the same target genes.

Consistent with the potential functional relevance of the selected modules, associated functional terms were found to comprise a range of biological processes relevant in a MND context. These include general cellular processes such as kinase signal transduction pathways,

regulation of the actin cytoskeleton, regulation of endocytosis, as well as neuron-specific processes such as learning and memory, and regulation of synapse assembly (Supplementary Data 7). Interestingly, differences in the impact of individual gene knockdowns were observed when comparing modules, which we propose to reflect some degree of functional specialization of the two ALS-related genes and the single SMA-associated gene (Fig. 3B). For example, the module related to "learning and memory" functions was strongly impacted by *caz* down-regulation, but to a lower extent by *Smn* or *TBPH* silencing. In contrast, the module "neuromuscular synaptic transmission" was strongly impacted by *TBPH*, followed by *caz*, and less so by *Smn* knockdown. Finally, some modules, like the one linked to "regulation of endocytosis" tended to be similarly impacted by all three knockdowns. Overall, the impact of *TBPH* and *Caz* knockdowns on functional modules is much more similar to each other than to *Smn*, which generally displays lower impact scores, with a few exceptions including "regulation of endocytosis" (Fig. 3B). This observation is quite striking considering that *Caz* and *TBPH* are associated to the same disease.

To determine the relevance of the selected modules to the pathophysiology of MNDs, we calculated for each module the percentage of proteins with human orthologs already linked to MNDs (according to the DisGeNET repository). Remarkably, selected modules were significantly enriched in proteins with MND-linked human orthologs when compared to modules that did not pass the "overall impact" threshold (p value = $1.5e-3$, Wilcoxon test) (Fig. 3C). This result suggests that we were able to identify novel disease-relevant interactions based on the convergent analysis of *Caz*, *Smn* and *TBPH*-dependent functional modules in *Drosophila*.

As the selected modules represent core biological functions regulated by the three proteins, we looked at the prevalence of direct targets (i.e. mRNAs identified by RIP-seq) among module components classified as DE and/or AS in the knockdown analysis. We found that 31% of the 411 DE/AS transcripts associated to selected modules are also bound by at least one of the three MND proteins. In non-selected modules, this number decreases significantly to 24% (p value = $1.4e-2$, Fig. 3D), being even lower for transcripts that do not integrate any functional module (18% of 2280 transcripts, p value = $3.1e-8$; Supplementary Data 7). Together, these results suggest that our integrated data analysis approach was able to identify key functional processes that are commonly and directly regulated by the three proteins. Our findings point to the ability of *Caz*, *Smn* and *TBPH* protein dysregulation to elicit a convergent functional impact through distinct individual targets. The connection to

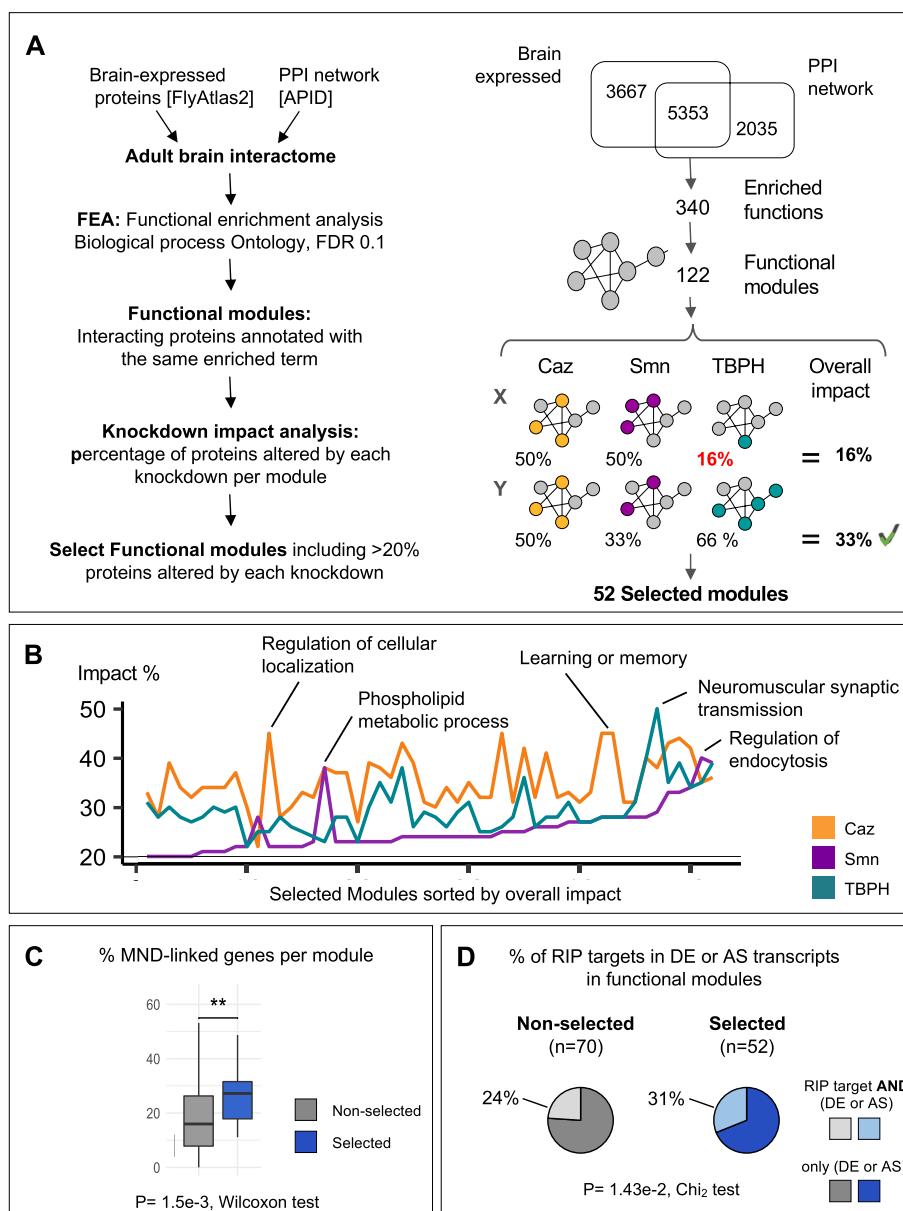


Fig. 3 Characterization of functional modules impacted by reduced abundance of Caz, Smn and TBPH proteins. **A** Left panel: workflow used to generate and select functional modules. The adult brain interactome was obtained from the APID protein-interaction network after filtering for proteins expressed in the adult *Drosophila* brain (i, see Methods). Functional enrichment analysis of the resulting interactome was performed to retrieve overrepresented GO Biological Processes (ii). Note that the functional enrichment returns all the proteins annotated in each overrepresented term. The modules were generated from the functional enrichment by retaining the proteins annotated and simultaneously interacting in the brain network (iii). Finally, the impact of *caz*, *smn* and *tbph* knockdown was evaluated for each module (iv) to select modules with >20% of transcripts altered in each individual knockdown (v). Right panel: summary the workflow outputs. “Overall impact” calculation is exemplified for two modules (X/Y) with the impact score indicated on the right. Only the Y module would be selected, as the overall impact of module X is below the defined threshold. **B** Line plot comparing the impact of individual knockdowns on selected modules, sorted by increasing overall impact. Modules with the highest impact for each protein are indicated by their short name. **C** Box plots showing the percentage of proteins with MND-linked orthologs in each module class. Selected modules (blue) are significantly enriched in proteins with MND-linked orthologs compared to non-selected modules (grey) (p value = 1.5e-3, Wilcoxon test). **D** Pie charts representing the fraction of transcripts with altered expression (DE) or splicing (AS) in response to a given protein knockdown that are simultaneously found in RNP complexes bound by the same protein. The high percentage of DE/AS transcripts (selected modules, blue pie chart) is significantly related to a higher frequency of DE/AS transcripts involved in RBPs bound by the same proteins (p-value = 5.4e-3, Chi² test of independence)

key biological processes is mediated by functional protein networks enriched in molecules with known links to MNDs. Further exploration of the selected networks may thus provide novel information to understand MND pathophysiology.

Convergent disruption of neuromuscular junction processes by altered Caz, TBPH or Smn protein levels

Pairwise comparison of the 52 selected modules revealed a high number of shared genes between many of them (see Supplementary Fig. S4). To generate a non-redundant map of the common functional networks established by Caz, Smn and TBPH, we coalesced groups of highly interconnected modules into larger but more condensed "super-modules" (Fig. 4). This resulted in seven

super-modules named after their core functional association: signaling, traffic, cytoskeleton, stress, behavior, synaptic transmission, and neuro-muscular junction (NMJ) (Supplementary Data 7). These super-modules range in size from 77 to 259 nodes, with a maximum overlap between any two super-modules of ~12% of the nodes (Supplementary Fig. S4). We next quantified the fraction of MND-associated gene orthologues in the different super-modules (MND-linked, Fig. 5, left panel). The super-modules related to behavior, neuro-muscular junction (NMJ) and cytoskeleton incorporated the largest fraction of MND-linked and AS transcripts. We further mapped the distribution of DE transcripts that are direct targets of Caz, Smn and TBPH (RNA-binding, Fig. 5, middle panel). Here, the super-modules related to

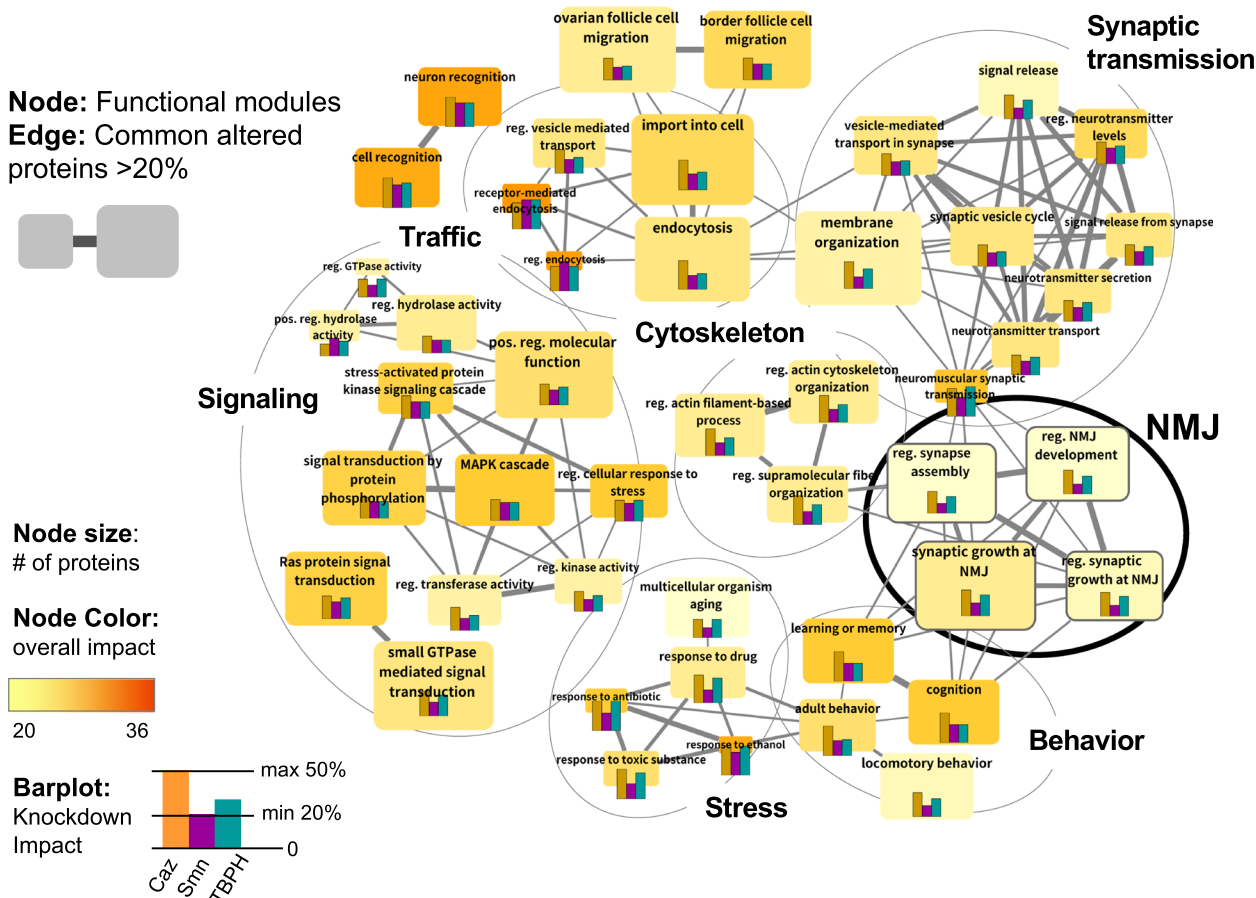


Fig. 4 Identification of functional super-modules through protein overlap analysis (A) Network representation of the selected functional modules. Nodes represent the selected modules designated by the original name of the gene ontology term. Node size indicates the number of proteins incorporated in the module and gradient color the overall impact, i.e., minimum % of transcripts altered by each knockdown, ranging between 20% (selection cut-off) and 36%. The bar plots within the nodes indicate the impact of each knockdown on the module (ranging from 20 to 50%). The height of the bars follows a linear scale that is preserved between plots, allowing for a comparison of the relative impact of individual genes on different modules. Overall and specific impact values for each module/gene are presented in Supplementary Data File 7. Edge width indicates the number of commonly altered transcripts between two modules. Modules were manually grouped into 7 "super-modules" (circles) based on edge density (common altered transcripts) and functional similarity of module names

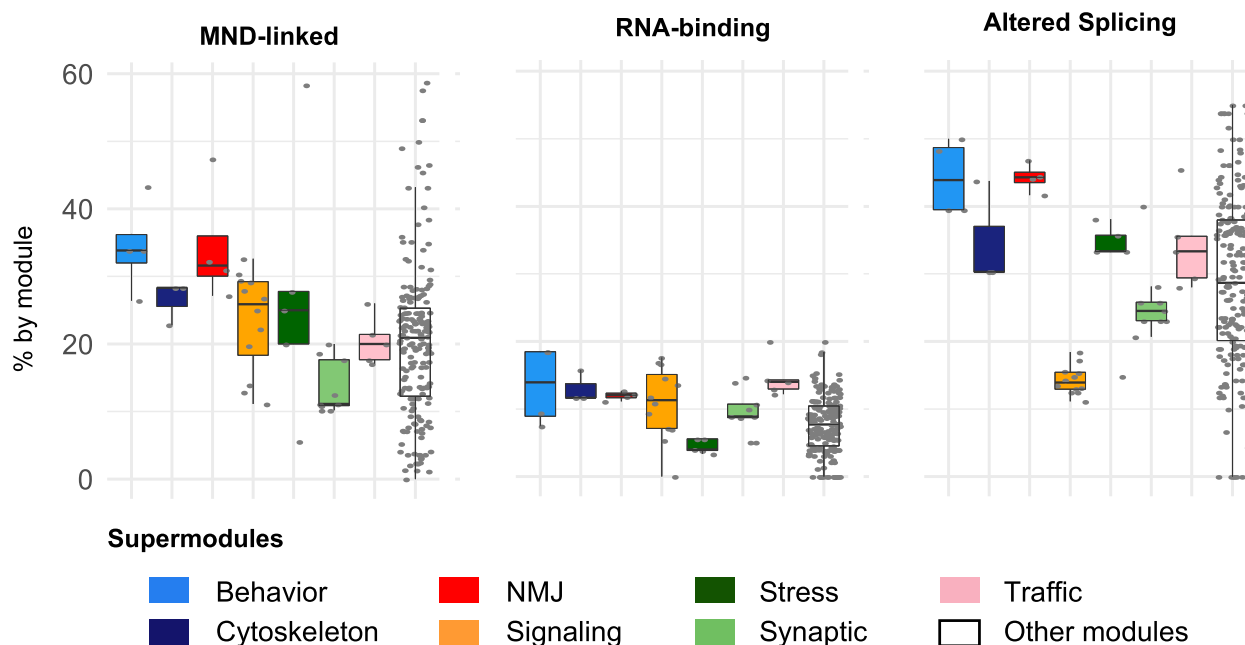


Fig. 5 Analysis of super-module features. Box plots showing the distribution of the percentage of annotated proteins in the modules composing the different super-modules (colored boxes) and across all other (non-selected) library modules (white boxes). Grey dots represent all the values for the individual modules that are part of each group. (Left) Percentage of proteins encoded by MND-linked gene orthologs according to the DisGeNET repository. (Middle) Percentage of proteins encoded by DE or AS transcripts that are direct RNA-binding targets of Caz, Smn or TBPH. (Right) Percentage of proteins encoded by transcripts with altered splicing patterns

behavior and traffic have a larger fraction of direct targets, highlighting the relevance of RNA-binding mechanisms in the regulation of these processes. Regulation through altered splicing (Altered Splicing, Fig. 5, right panel), on the other hand, is more frequent in modules related with behavior, NMJ, stress and cytoskeleton. Given the critical link between MNDs and the physiology of NMJs, we focused on the NMJ super-module for a more in-depth analysis.

The NMJ super-module comprises 104 proteins, of which 49% (51 nodes) are encoded by genes differentially expressed and/or displaying altered splicing in at least one knockdown condition (Supplementary Data 8). 38 of these genes establish direct interactions, forming the subnetwork represented in Fig. 6A. To assess the degree to which the NMJ “super module” functionally interacts with Caz, Smn and TBPH *in vivo*, we cross-referenced it to genetic modifiers of *Drosophila* Smn, Caz or TBPH mutants identified in genome-wide screens for modulators of degenerative phenotypes using the Exelixis transposon collection (Kankel et al. 2020, Sen et al. 2013, Chang et al. 2008). Interestingly, 21 nodes (~20%) of the NMJ “super module” were identified as either suppressors or enhancers of these models of neurodegeneration (Supplementary Data 8). Given that the reported percentage of recovered modifiers in these screens ranged

between 2 and 5%, this result highlights the biological relevance of the functional modules identified through our approach.

Detailed analysis of the FlyBase annotations for the genes within the NMJ subnetwork represented in Fig. 6A provides interesting insights into the potential mechanisms causing neuronal dysfunction in the context of MNDs.

First, essential genes are highly overrepresented in the module. While about 30% of *Drosophila* genes are expected to be essential for adult viability [70], more than 75% of genes present in the NMJ super-module have a lethal phenotype (Fig. 6B). Exceptions are *CASK*, *liprin-γ*, *Nlg2*, *metro*, *dbo* and *nwk*. For *RhoGAP92B* and *Nrx-1*, it is so far not entirely clear whether mutant alleles would cause lethality.

We next asked whether the human orthologs of these genes are linked to neurological disorders. *TBPH* (TDP-43), *unc-104* (KIF1A, B, C), *Ank2* (Ank2), *futsch* (MAP1A/B), *sgg* (GSK3A/B), *Src64B* (FYN/SRC) and *Nrx-1* (Nrx-1–3) have been implicated in MNDs (hexagonal nodes in network). Moreover, a high number of genes have human orthologs linked to other neuronal dysfunctions or diseases. For example, human orthologs to fly genes *CASK* (CASK), *Mnb* (DYRK1A), *Dlg-1* (DLG1), *Cdc42* (CDC42), *Fmr1* (FMR1, FXR1/2), *trio* (TRIO),

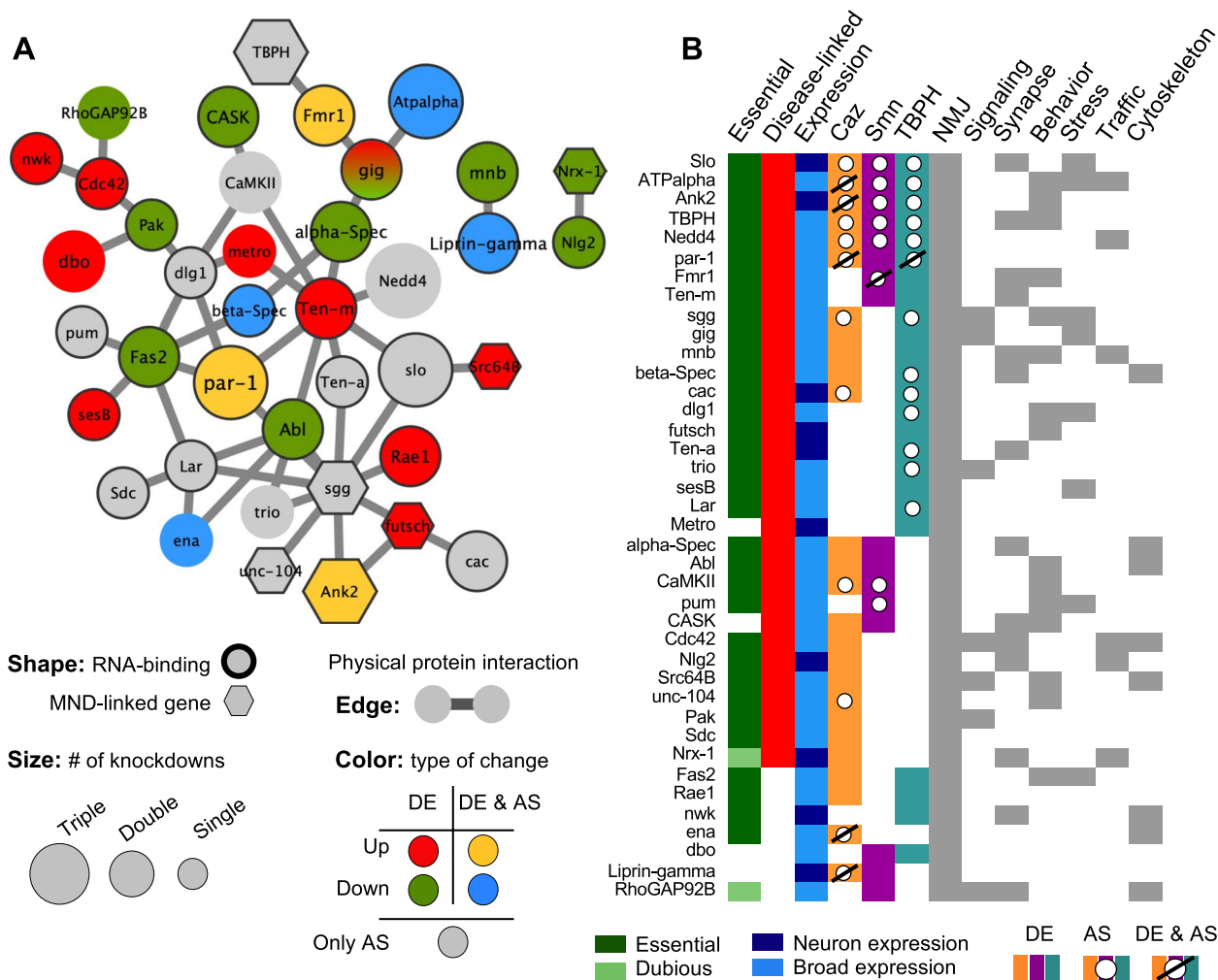


Fig. 6 The neuro-muscular junction (NMJ) super-module. **A** Protein-interaction subnetwork of NMJ super-module nodes that are encoded by transcripts altered by knockdown of *Caz*, *Smn* and/or *TBPH*. Only proteins with direct interaction with other proteins encoded by DE/AS transcripts are represented. Node size indicates the number of knockdown models in which the transcript revealed altered expression (DE) and/or altered splicing (AS). Red and green nodes are encoded by transcripts presenting upregulation or downregulation, respectively; a red-green gradient is used to represent nodes encoded by transcripts with discordant DE changes in two knockdowns; several transcripts are both DE and AS, represented either as yellow (upregulated and AS) or blue (downregulated and AS) nodes; grey nodes indicate transcripts only showing AS. Bold outline highlights proteins encoded by transcripts identified in the RIP-Seq analysis (labeled “RNA-binding”). Hexagons highlight proteins with MND-linked human orthologs. **B** Categorical heat map summarizing data concerning the proteins/genes within the network represented in A. Essential proteins were defined according to the FlyBase repository. Proteins labeled as “Dubious” display a lethal phenotype after induction of RNAi. Thus, it is likely that flies homozygous for amorphic mutations would result in lethality during development. However, since this might result from off-target effects, they were not considered essential. MND-associations were retrieved from the DisGeNET repository. *Caz*, *Smn* and *TBPH* columns indicate in which knockdown models the corresponding transcripts were found altered; different codes are used to highlight the DE, DE + AS or AS only nature of the change. Last 7 columns indicate whether the protein is also found in other super-modules

Nedd4 (NEDD4L/NEDD4) and *CamKII* (CAMK2A/B/D) have been linked to intellectual disability. Epilepsy has been associated with mutations in the human gene orthologs of *cac* (CACNA1A/B/E), *alpha-Spec* (SPTAN1) and *slo* (KCNMA1). In addition, human psychiatric diseases like schizophrenia or bipolar disorder can be caused by alterations in genes with high similarity to *Pak* (PAK1/2/3) and *dbo* (KLHL20 indirect, via regulation

of *Pak*, [71]). Alterations in the human gene coding Teneurin Transmembrane Protein 4 (TENM4, shares high homology with fly *Ten-a* and *Ten-m*) are known to cause hereditary essential tremor-5, while human neuroligins NLGN1, NLGN3 and NLGN4X were linked to autism/Asperger syndrome and encode orthologs to fly *Nlg2*. Finally, alterations in human orthologs to fly *Pum* (PUM1/2), *beta-Spec* (SPTBN1/2) and *Ank2* (ANK1/2/3

have been associated with Ataxia-like phenotypes and mental retardation. In total, we were able to find direct associations to human MN or neurological disorders for 32 out of the 39 represented genes. Thus, although most of the genes captured in our analysis are not exclusively expressed in neurons, their mutations are somehow associated to abnormal neuroanatomy and function. Interestingly, this holds true for the non-essential genes as well. It is also noteworthy that, in spite of the relatively limited overlap between the different super-modules, all the proteins that constitute this core NMJ network are common to at least another super-module, and on average to more than half of them (Fig. 6B).

Altogether, these observations imply that the proteins encoded by the NMJ super-module genes fulfill relevant functions in NMJ maintenance and that their alteration could eventually contribute to MND. Our results reveal that *Caz*, *Smn* and *TBPH* act in concert to regulate biological processes linked to NMJ maturation and function by altering the expression of transcripts encoding distinct, yet physically and functionally interacting proteins. We propose that the functional complexes established by these proteins may represent important players in disease progression, emerging as potential common therapeutic targets rather than the individual proteins that compose them.

Discussion

SMA and ALS are the most common MNDs and are characterized by a progressive degeneration of motor neurons and loss of skeletal muscle innervation. Although both diseases share many pathological features, including selective motor neuron vulnerability, altered neuronal excitability, as well as pre- and post-synaptic NMJ defects [26], their very different genetic origins and onset led them to be classified as independent, non-related diseases. This view has been challenged by recent studies demonstrating that disease-causing proteins (*Smn* for SMA, *Fus* and *TDP-43* for ALS) are connected through both molecular and genetic interactions (reviewed by [4]). Furthermore, the increasing number of functions attributed to these proteins converges onto common regulatory processes, among which control of transcription and splicing in the nucleus, as well as mRNA stability and subcellular localization in the cytoplasm. Despite the observed convergence in the molecular function of *Smn*, *Fus* and *TDP-43*, transcripts co-regulated by these three proteins, and thus central to SMA and ALS pathophysiology, have not been identified by previous transcriptomic analyses. In this study, we used the power of *Drosophila* to systematically identify, on one hand the mRNA repertoires bound by each protein in the nucleus and cytoplasm of adult neurons and, on the other hand, the mRNA populations undergoing significant alterations

in steady-state levels or splicing as a consequence of the knockdown of each protein. This approach revealed a striking absence of mRNAs commonly bound by the three proteins and a small, albeit significant, number of commonly altered transcripts. Notwithstanding, and contrary to the simplest model that explains shared disease phenotypes, this subset of shared transcripts did not present any functional signature linking it to biological pathways related to disease progression.

Considering that functional protein complexes are at the core of all critical cellular mechanisms, an alternative model posits that shared phenotypes may arise through convergent effects on independent elements of such complexes. To investigate this possibility, we mapped the de-regulated transcripts identified in our transcriptomic analysis onto a comprehensive and non-biased library of neuronal physically interacting and functionally collaborating protein consortia. Following our recently published approach [69], definition of these functional units was achieved through the integration publicly available information from *Drosophila* PPI networks, neuronal gene expression and gene ontology annotations. This approach led to the identification of a set of 52 functional modules significantly impacted by all three proteins through the regulation of distinct components (Fig. 3). Of note, although we used as selection criterium the presence of a minimum of 20% of module elements displaying altered gene expression in each knock-down model, we found that modules passing this cut-off were significantly enriched in direct RNA binding targets of *Smn*, *Caz* and *TBPH* compared to non-selected modules (Fig. 3D). Considering that only a very small proportion of these targets are common to the three proteins, this observation underscores our hypothesis of convergent regulation of functional complexes through distinct individual elements. Furthermore, the enrichment of RIP targets in the selected modules establishes a direct mechanistic link between changes in the levels of *Smn*, *Caz* and *TBPH* and changes in the steady state expression of module components. It is possible that the steady-state levels of transcripts encoding other proteins that belong to the same complex will vary as part of homeostatic feed-back processes. This could justify the presence of a relatively large number of DE/AS genes that are common to the three knockdown models, but whose transcripts are not found as direct protein targets in our RIP-seq data.

The functional classification of the 52 selected modules revealed a striking connection with critical pathways for MND. Particularly relevant, mapping of the human orthologues of the different module components revealed a high number of genes with reported association to MNDs. This observation provides support to the relevance of our approach, which uses *Drosophila* as a model for uncovering

molecular interactions underlying human disease. It is noteworthy that the enrichment in disease-associated orthologues was not homogeneous across the super-modules generated by coalescing highly related modules into a smaller number of larger functional protein consortia (Fig. 5). Interestingly, we found that a super-module related to NMJ function was among the highest scoring regarding both enrichment in MND associated genes and presence of alternatively spliced/direct RNA binding targets. The subset of DE/AS genes present in this module forms a highly interconnected network and the analysis of FlyBase annotations for this focused subset provided interesting insights into potential mechanisms that may underlie neuronal dysfunction. An unusually large number of DE/AS genes within the NMJ super-module was found to correspond to essential genes, indispensable for the development of adult flies. Alterations in the abundance and/or function of these genes have been linked in several cases to a disturbance of nervous system function. This is reflected by an alteration in stress response and/or abnormal behavior in either embryos, larvae or adult flies. Strikingly, even the non-lethal genes captured in this super-module have been shown to impact nervous system development and cause abnormal neuroanatomy when mutated/silenced.

The essential function of most of the selected genes obviously prohibits the analysis of loss-of-function phenotypes in the adult organism. In neurons, classical forward and reverse genetics of essential genes and clonal analysis is complex. This is the reason why there is little genetic data on gene products involved in neuronal maintenance. Conditional knockouts and spatiotemporal control of RNAi-mediated gene silencing (like the approach used here) is a way to overcome these limitations. We can only speculate whether a neuron specific, adult-onset knock-down of the individual genes within the super-module will impair adult neuron integrity. However, it is reasonable to assume that the collective deregulation of this set of genes within the super-module is incompatible with proper neuronal function. This assumption is particularly sound if the encoded proteins and their associated functional complexes are found to contribute to cellular processes critical for neurons, as indeed we find in this case. In fact, for almost all proteins encoded by the NMJ sub-network, synaptic functions have been reported. Interestingly, the other identified super-modules are also functionally annotated to cellular mechanisms that are especially important in neurons, like signaling, cytoskeletal dynamics, traffic and transport. Thus, an attractive model emerges for SMA and ALS MN dysfunction: convergent functional impacts can emerge from the independent, subtle deregulation of a group of proteins that are part of a set connected, neuronal functional modules. A persisting impairment in critical neuronal processes could initiate a self-reinforcing

cycle of detrimental events, eventually resulting in neuronal decline. Especially in the case of sporadic, late-onset ALS, this model would comply with the events observed in disease progression.

In conclusion, our work revealed common functional modules that are under the control of the SMA and ALS disease-associated gene orthologues *Smn*, *TBPH* and *caz*. This control is exerted through distinct target genes that encode proteins which collaborate in neuronal functional consortia. The fact that these modules are deregulated in asymptomatic disease models and are primarily composed of ubiquitously expressed genes opens an interesting avenue of research regarding the discovery of novel disease biomarkers. Importantly, the identification of convergent molecular dysfunctions linked to distinct MND-associated genes suggests that common therapeutic strategies able to help slowdown disease progression or improve symptoms may exist, in spite of the diversity of genetic backgrounds.

Abbreviations

ALS	Amyotrophic Lateral Sclerosis
AS	Alternative Splicing
DE	Differentially Expressed
FC	Fold Change
GFP	Green Fluorescent Protein
GO	Gene Ontology
MN	Motor Neuron
MND	Motor Neuron Disease
NMJ	Neuromuscular Junction
RBP	RNA Binding Protein
RIP	RNA Immuno-Precipitation
RNAi	RNA interference
RNA-seq	RNA sequencing
RNP	Ribonucleoprotein
PPI	Protein-Protein-Interaction
shRNA	Short hairpin RNA
SMA	Spinal Muscular Atrophy

Supplementary Information

The online version contains supplementary material available at <https://doi.org/10.1186/s12864-023-09562-4>.

Additional file 1. Supplementary Dataset file 1.

Additional file 2. Supplementary Dataset file 2.

Additional file 3. Supplementary Dataset file 3.

Additional file 4. Supplementary Dataset file 4.

Additional file 5. Supplementary Dataset file 5.

Additional file 6. Supplementary Dataset file 6.

Additional file 7. Supplementary Dataset file 7.

Additional file 8. Supplementary Dataset file 8.

Additional file 9. Supplementary Information.

Acknowledgements

The authors would like to acknowledge Jörg B. Schulz and Joachim Weiss for support and helpful discussions during the course of the project. We thank the Genomics Core Facility (EMBL, Germany) for assistance with library preparation from RIP samples and sequencing.

Authors' contributions

MG-C, AV, FB, and JDJLR conceptualized the research approach and supervised the research work; BF validated and generated the RNAi samples; MH generated and characterized the GFP-tagged lines and did the RNA-IP assays; LP assessed the functionality of GFP-tagged lines; MP and TMM did the RNA-seq data analysis; MG-V developed the methods and performed the network-based analysis; FRP contributed to the conceptualization and development of the network analysis. MG-C, AV, FB and MG-V wrote the manuscript draft. FRP, MG-C and MG-V did the final manuscript revisions. All authors read and approved the final manuscript.

Funding

This work is part of an EU Joint Programme – Neurodegenerative Disease Research (JPND) project with the acronym 'Fly-SMALS'. The project is supported through the following funding organisations under the aegis of JPND – www.jpnd.eu: France, Agence Nationale de la Recherche; Germany, Bundesministerium für Bildung und Forschung (BMBF); Portugal, Fundação para a Ciência e a Tecnologia and Spain, Instituto de Salud Carlos III (ISCIII). Associated to the JPND, the group of JDJLR was funded for this work by the ISCIII and FEDER through projects AC14/00024 and PI15/00328. Work in MG-C's group was supported by the grant JPND-CD/0002/2013 and by UIDB/04046/2020 and UIDP/04046/2020 Centre grants from FCT, Portugal (to BiolSI). Work in F.B.'s group is supported by the ANR (through the MEMORNP research grant and the 'Investments for the Future' LABEX SIGNALIFE program # ANR-11-LABX-0028-01). MG-V and TMM are recipients of a fellowship from the BioSys PhD programme PD65-2012 (Refs PD/BD/128109/2016 and PD/BD/142854/2018, respectively) from FCT (Portugal).

Availability of data and materials

The datasets generated and/or analyzed during the current study are available in the European Nucleotide Archive repository under the umbrella study Fly-SMALS, with accession numbers PRJEB42797 (<https://www.ebi.ac.uk/ena/browser/view/PRJEB42797>) and PRJEB42798 (<https://www.ebi.ac.uk/ena/browser/view/PRJEB42798>).

Declarations

Ethical approval and consent to participate

Not applicable.

Consent for publication

Not applicable.

Competing interests

The authors declare no competing interests.

Author details

¹BiolSI – Institute for Biosystems and Integrative Sciences, Faculty of Sciences, University of Lisbon, 1749-016 Lisbon, Portugal. ²Department of Medicine and Cytometry General Service-15 Nucleus, Cancer Research Centre (IBMCC/CSIC/USAL/IBSAL), CIBERONC, 16 37007, Salamanca, Spain. ³Institut de Biologie Valrose, Université Côte d'Azur, CNRS, 06108 Nice, Inserm, France. ⁴Department of Neurology, Medical Faculty, RWTH Aachen University, 52074 Aachen, Germany. ⁵Cancer Research Center (CiC-IBMCC, CSIC/USAL/IBSAL), Consejo Superior de Investigaciones Científicas (CSIC) and University of Salamanca (USAL), 37007 Salamanca, Spain. ⁶JARA-BRAIN Institute Molecular Neuroscience and Neuroimaging, Forschungszentrum Jülich GmbH RWTH Aachen University, 52074 Aachen, Germany.

Received: 6 May 2023 Accepted: 8 August 2023

Published online: 27 September 2023

References

- Achsel T, Barabino S, Cozzolino M, Carri MT. The intriguing case of motor neuron disease: ALS and SMA come closer. *Biochem Soc Trans*. 2013;41:1593–7.
- Ling S-C, Polymenidou M, Cleveland DW. Converging mechanisms in ALS and FTD: disrupted RNA and protein homeostasis. *Neuron*. 2013;79:416–38.
- Taylor JP, Brown RH, Cleveland DW. Decoding ALS: from genes to mechanism. *Nature*. 2016;539:197–206.
- Gama-Carvalho M, Garcia-Vaquero ML, Pinto FR, Besse F, Weis J, Voigt A, et al. Linking amyotrophic lateral sclerosis and spinal muscular atrophy through RNA-transcriptome homeostasis: a genomics perspective. *J Neurochem*. 2017;141:12–30.
- Zaepfel BL, Rothstein JD. RNA Is a Double-Edged Sword in ALS Pathogenesis. *Front Cell Neurosci*. 2021;15: 708181.
- Li DK, Tisdale S, Lotti F, Pellizzoni L. SMN control of RNP assembly: From post-transcriptional gene regulation to motor neuron disease. *Semin Cell Dev Biol*. 2014;32:22–9.
- Price PL, Morderer D, Rossoll W. RNP Assembly Defects in Spinal Muscular Atrophy. *Adv Neurobiol*. 2018;20:143–71.
- Boulisfane N, Choleza M, Rage F, Neel H, Soret J, Bordonné R. Impaired minor tri-snRNP assembly generates differential splicing defects of U12-type introns in lymphoblasts derived from a type I SMA patient. *Hum Mol Genet*. 2010;20:641–8.
- Workman E, Kolb SJ, Battle DJ. Spliceosomal small nuclear ribonucleoprotein biogenesis defects and motor neuron selectivity in spinal muscular atrophy. *Brain Res*. 2012;1462:93–9.
- Tisdale S, Lotti F, Saieva L, Meerbeke JPV, Crawford TO, Sumner CJ, et al. SMN Is Essential for the Biogenesis of U7 Small Nuclear Ribonucleoprotein and 3'-End Formation of Histone mRNAs. *Cell Rep*. 2013;5:1187–95.
- Donlin-Asp PG, Bassell GJ, Rossoll W. A role for the survival of motor neuron protein in mRNP assembly and transport. *Curr Opin Neurobiol*. 2016;39:53–61.
- Donlin-Asp PG, Fallini C, Campos J, Chou C-C, Merritt ME, Phan HC, et al. The Survival of Motor Neuron Protein Acts as a Molecular Chaperone for mRNP Assembly. *Cell Rep*. 2017;18:1660–73.
- Pellizzoni L, Charroux B, Rappasilber J, Mann M, Dreyfuss G. A functional interaction between the survival motor neuron complex and RNA polymerase II. *J Cell Biol*. 2001;152:75–85.
- Zou J, Barahmand-pour F, Blackburn ML, Matsui Y, Chansky HA, Yang L. Survival Motor Neuron (SMN) Protein Interacts with Transcription Corepressor mSin3A*. *J Biol Chem*. 2004;279:14922–8.
- Zhang Z, Lotti F, Dittmar K, Younis I, Wan L, Kasim M, et al. SMN deficiency causes tissue-specific perturbations in the repertoire of snRNAs and widespread defects in splicing. *Cell*. 2008;133:585–600.
- Zhao DY, Gish G, Braunschweig U, Li Y, Ni Z, Schmitges FW, et al. SMN and symmetric arginine dimethylation of RNA polymerase II C-terminal domain control termination. *Nature*. 2016;529:48–53.
- Fallini C, Zhang H, Su Y, Silani V, Singer RH, Rossoll W, et al. The Survival of Motor Neuron (SMN) Protein Interacts with the mRNA-Binding Protein HuD and Regulates Localization of Poly(A) mRNA in Primary Motor Neuron Axons. *J Neurosci*. 2011;31:3914–25.
- Fallini C, Donlin-Asp PG, Rouanet JP, Bassell GJ, Rossoll W. Deficiency of the Survival of Motor Neuron Protein Impairs mRNA Localization and Local Translation in the Growth Cone of Motor Neurons. *J Neurosci*. 2016;36:3811–20.
- Cruz SD, Cleveland DW. Understanding the role of TDP-43 and FUS/TLS in ALS and beyond. *Current opinion in neurobiology*. 2011;21(6):904–19.
- Ratti A, Buratti E. Physiological functions and pathobiology of TDP-43 and FUS/TLS proteins. *J Neurochem*. 2016;138(Suppl 1):95–111.
- Ederle H, Dormann D. TDP-43 and FUS en route from the nucleus to the cytoplasm. *FEBS Lett*. 2017;591:1489–507.
- Birsa N, Benthamp MP, Fratta P. Cytoplasmic functions of TDP-43 and FUS and their role in ALS. *Semin Cell Dev Biol*. 2020;99:193–201.
- Zbinden A, Pérez-Berlanga M, Rossi PD, Polymenidou M. Phase Separation and Neurodegenerative Diseases: A Disturbance in the Force. *Dev Cell*. 2020;55:45–68.
- Li YR, King OD, Shorter J, Gitler AD. Stress granules as crucibles of ALS pathogenesis. *J Cell Biol*. 2013;201:361–72.
- Fernandes N, Eshleman N, Buchan JR. RNA Metabolism in Neurodegenerative Diseases. *Adv Neurobiol*. 2018;20:173–212.
- Bowerman M, Murray LM, Scamps F, Schneider BL, Kothary R, Raoul C. Pathogenic commonalities between spinal muscular atrophy and amyotrophic lateral sclerosis: Converging roads to therapeutic development. *Eur J Méd Genet*. 2018;61:685–98.
- Yamazaki T, Chen S, Yu Y, Yan B, Haertlein TC, Carrasco MA, et al. FUS-SMN protein interactions link the motor neuron diseases ALS and SMA. *Cell Rep*. 2012;2:799–806.

28. Groen EJM, Fumoto K, Blokhuis AM, Engelen-Lee J, Zhou Y, van den Heuvel DMA, et al. ALS-associated mutations in FUS disrupt the axonal distribution and function of SMN. *Hum Mol Genet.* 2013;22:3690–704.
29. Tsujii H, Iguchi Y, Furuya A, Kataoka A, Hatsuta H, Atsuta N, et al. Spliceosome integrity is defective in the motor neuron diseases ALS and SMA. *EMBO Mol Med.* 2013;5:221–34.
30. Sun S, Ling S-C, Qiu J, Albuquerque CP, Zhou Y, Tokunaga S, et al. ALS-causative mutations in FUS/TLS confer gain and loss of function by altered association with SMN and U1-snRNP. *Nat Commun.* 2015;6:6171.
31. Perera ND, Sheehan RK, Crouch PJ, White AR, Horne MK, Turner BJ. Enhancing survival motor neuron expression extends lifespan and attenuates neurodegeneration in mutant TDP-43 mice. *Hum Mol Genet.* 2016;25:4080–93.
32. Chi B, O'Connell JD, Iocolano AD, Coady JA, Yu Y, Gangopadhyay J, et al. The neurodegenerative diseases ALS and SMA are linked at the molecular level via the ASC-1 complex. *Nucleic Acids Res.* 2018;46:11939–51.
33. Cacciottolo R, Ciantar J, Lanfranco M, Borg RM, Vassallo N, Bordonné R, et al. SMN complex member Gemin3 self-interacts and has a functional relationship with ALS-linked proteins TDP-43, FUS and Sod1. *Sci Rep.* 2019;9:18666.
34. Lagier-Tourenne C, Polymenidou M, Hutt KR, Vu AQ, Baughn M, Huelga SC, et al. Divergent roles of ALS-linked proteins FUS/TLS and TDP-43 intersect in processing long pre-mRNAs. *Nat Neurosci.* 2012;15:1488–97.
35. Kline RA, Kaifer KA, Osman EY, Carella F, Tiberi A, Ross J, et al. Comparison of independent screens on differentially vulnerable motor neurons reveals alpha-synuclein as a common modifier in motor neuron diseases. *PLoS Genet.* 2017;13: e1006680.
36. Wang J-W, Brent JR, Tomlinson A, Shneider NA, McCabe BD. The ALS-associated proteins FUS and TDP-43 function together to affect Drosophila locomotion and life span. *J Clin Invest.* 2011;121:4118–26.
37. McGurk L, Berson A, Bonini NM. Drosophila as an In Vivo Model for Human Neurodegenerative Disease. *Genetics.* 2015;201:377–402.
38. Aquilina B, Cauchi RJ. Genetic screen identifies a requirement for SMN in mRNA localisation within the Drosophila oocyte. *BMC Res Notes.* 2018;11:378.
39. Olesnick E, Wright E. Drosophila as a Model for Assessing the Function of RNA-Binding Proteins during Neurogenesis and Neurological Disease. *J Dev Biol.* 2018;6:21.
40. Spring AM, Raimer AC, Hamilton CD, Schillinger MJ, Matera AG. Comprehensive Modeling of Spinal Muscular Atrophy in Drosophila melanogaster. *Front Mol Neurosci.* 2019;12:113.
41. Liguori F, Amadio S, Volonté C. Fly for ALS: Drosophila modeling on the route to amyotrophic lateral sclerosis modifiers. *Cell Mol Life Sci.* 2021;78:6143–60.
42. Chang HCH, Dimlich DN, Yokokura T, Mukherjee A, Kankel MW, Sen A, et al. Modeling spinal muscular atrophy in Drosophila. *PLoS one.* 2008;3:e3209.
43. Kankel MW, Sen A, Lu L, Theodorou M, Dimlich DN, McCampbell A, et al. Amyotrophic Lateral Sclerosis Modifiers in Drosophila Reveal the Phospholipase D Pathway as a Potential Therapeutic Target. *Genetics.* 2020;215:747–66.
44. Vijayakumar J, Perrois C, Heim M, Bousset L, Alberti S, Besse F. The prion-like domain of Drosophila Imp promotes axonal transport of RNP granules in vivo. *Nat Commun.* 2019;10:2593.
45. Amaral AJ, Brito FF, Chobanyan T, Yoshikawa S, Yokokura T, Vactor DV, et al. Quality assessment and control of tissue specific RNA-seq libraries of Drosophila transgenic RNAi models. *Front Genet.* 2014;5:43.
46. dos Santos G, Schroeder AJ, Goodman JL, Strelets VB, Crosby MA, Thurmond J, et al. FlyBase: introduction of the Drosophila melanogaster Release 6 reference genome assembly and large-scale migration of genome annotations. *Nucleic Acids Res.* 2015;43:D690–7.
47. Dobin A, Davis CA, Schlesinger F, Drenkow J, Zaleski C, Jha S, et al. STAR: ultrafast universal RNA-seq aligner. *Bioinformatics (Oxford, England).* 2013;29:15–21.
48. Love MI, Huber W, Anders S. Moderated estimation of fold change and dispersion for RNA-seq data with DESeq2. *Genome Biol.* 2014;15:550.
49. Huber W, Carey VJ, Gentleman R, Anders S, Carlson M, Carvalho BS, et al. Orchestrating high-throughput genomic analysis with Bioconductor. *Nat methods.* 2014;12:115–21.
50. Ritchie ME, Phipson B, Wu D, Hu Y, Law CW, Shi W, et al. limma powers differential expression analyses for RNA-sequencing and microarray studies. *Nucleic Acids Res.* 2015;43:e47–e47.
51. Law CW, Chen Y, Shi W, Smyth GK. voom: precision weights unlock linear model analysis tools for RNA-seq read counts. *Genome Biol.* 2014;15:R29–R29.
52. Shen S, Park JW, Lu Z, Lin L, Henry MD, Wu YN, et al. rMATS: Robust and flexible detection of differential alternative splicing from replicate RNA-Seq data. *Proc Natl Acad Sci.* 2014;111:E5593–601.
53. Leader DP, Krause SA, Pandit A, Davies SA, Dow JAT. FlyAtlas 2: a new version of the Drosophila melanogaster expression atlas with RNA-Seq, miRNA-Seq and sex-specific data. *Nucleic Acids Res.* 2017;46 Database issue:gx976.
54. Wickham H. ggplot2: Elegant Graphics for Data Analysis. New York: Springer-Verlag; 2016.
55. Wang M, Zhao Y, Zhang B. Efficient Test and Visualization of Multi-Set Intersections. *Sci Rep-uk.* 2015;5:16923.
56. Alonso-López D, Campos-Laborie FJ, Gutiérrez MA, Lambourne L, Calderwood MA, Vidal M, et al. APID database: redefining protein–protein interaction experimental evidences and binary interactomes. *Database: J Biol Databases Curation.* 2019;2019:baz005.
57. Alonso-López D, Gutiérrez MA, Lopes KP, Prieto C, Santamaría R, Rivas JDL. APID interactomes: providing proteome-based interactomes with controlled quality for multiple species and derived networks. *Nucleic Acids Res.* 2016;44:W529–35.
58. Mora A, Donaldson IM. iRefR: an R package to manipulate the iRefIndex consolidated protein interaction database. *BMC Bioinform.* 2011;12:455–455.
59. Grote S. GOfuncR: Gene ontology enrichment using FUNC - R package version 1.19.0. 2020.
60. Grice SJ, Liu J-L. Survival Motor Neuron Protein Regulates Stem Cell Division, Proliferation, and Differentiation in Drosophila. *PLoS Genet.* 2011;7: e1002030.
61. Xia R, Liu Y, Yang L, Gal J, Zhu H, Jia J. Motor neuron apoptosis and neuromuscular junction perturbation are prominent features in a Drosophila model of Fus-mediated ALS. *Mol Neurodegener.* 2012;7:10.
62. Cragnaz L, Klima R, Skoko N, Budini M, Feiguin F, Baralle FE. Aggregate formation prevents dTDP-43 neurotoxicity in the Drosophila melanogaster eye. *Neurobiol Dis.* 2014;71:74–80.
63. McGuire SE, Le PT, Osborn AJ, Matsumoto K, Davis RL. Spatiotemporal Rescue of Memory Dysfunction in Drosophila. *Science.* 2003;302:1765–8.
64. Liu J-L, Gall JG. U bodies are cytoplasmic structures that contain uridine-rich small nuclear ribonucleoproteins and associate with P bodies. *Proc Natl Acad Sci.* 2007;104:11655–9.
65. Cauchi RJ, Sanchez-Pulido L, Liu J-L. Drosophila SMN complex proteins Gemin2, Gemin3, and Gemin5 are components of U bodies. *Exp Cell Res.* 2010;316:2354–64.
66. Mili S, Steitz JA. Evidence for reassociation of RNA-binding proteins after cell lysis: Implications for the interpretation of immunoprecipitation analyses. *RNA.* 2004;10:1692–4.
67. Osterwalder T, Yoon KS, White BH, Keshishian H. A conditional tissue-specific transgene expression system using inducible GAL4. *Proc Natl Acad Sci.* 2001;98:12596–601.
68. Scialo F, Sriram A, Stefanatos R, Sanz A. Practical Recommendations for the Use of the GeneSwitch Gal4 System to Knock-Down Genes in Drosophila melanogaster. *PLoS ONE.* 2016;11: e0161817.
69. García-Vaquero ML, Gama-Carvalho M, Pinto FR, Rivas JDL. Biological interacting units identified in human protein networks reveal tissue-functional diversification and its impact on disease. *Comput Struct Biotechnology J.* 2022;20:3764–78.
70. Spradling AC, Stern D, Beaton A, Rhem EJ, Laverty T, Mozden N, et al. The Berkeley Drosophila Genome Project Gene Disruption Project: Single P-Element Insertions Mutating 25% of Vital Drosophila Genes. *Genetics.* 1999;153:135–77.
71. Wang M, Chen P-Y, Wang C-H, Lai T-T, Tsai P-I, Cheng Y-J, et al. Dbo/Henji Modulates Synaptic dPAK to Gate Glutamate Receptor Abundance and Postsynaptic Response. *PLoS Genet.* 2016;12: e1006362.

Publisher's Note

Springer Nature remains neutral with regard to jurisdictional claims in published maps and institutional affiliations.